

Impact of Perturbations on Watersheds

E. Fehr,^{1,*} D. Kadau,¹ J. S. Andrade Jr.,^{1,2} and H. J. Herrmann^{1,2}

¹*IfB, ETH Zürich, 8093 Zürich, Switzerland*

²*Departamento de Física, Universidade Federal do Ceará, 60451-970 Fortaleza, Ceará, Brazil*

We find that watersheds in real and artificial landscapes can be strongly affected by small, local perturbations like landslides or tectonic motions. We observe power-law scaling behavior for both the distribution of areas enclosed by the original and the displaced watershed as well as the probability density to induce, after perturbation, a change at a given distance. Scaling exponents for real and artificial landscapes are determined, where in the latter case the exponents depend linearly on the Hurst exponent of the applied fractional Brownian noise. The obtained power-laws are shown to be independent on the strength of perturbation. Theoretical arguments relate our scaling laws for uncorrelated landscapes to properties of invasion percolation.

PACS numbers: 64.60.ah, 91.10.Jf, 89.75.Da, 92.40.Cy

Watersheds are the lines separating adjacent drainage basins (catchments) and play, hence, a fundamental role in water management [1], landslides [2, 3] and flood prevention [3, 4]. Since ancient times watersheds have been used to delimit boundaries and have already become issues in disputes between countries [5]. Moreover, similar problems also appear in other areas such as Image Processing and Medicine [6], which shows the generality and importance to fully understand the subtle dynamical properties of watersheds. But how sensitive are watersheds to slight localized modifications of the landscapes? Can these perturbations produce large, non-local changes in the watershed? Geographers and geomorphologists have studied the evolution of watersheds in time and found it to be driven by local events called stream capture. These events can affect the biogeography [7], and occur due to erosion, natural damming, tectonic motion as well as volcanic activity [8–11]. Recently, the associated relevant mechanisms were investigated numerically and in small scale experiments [12]. Finally, the problem studied here is also of interest to image processing, in order to circumvent segmentation failure [13].

In this Letter we investigate the effects of topological modifications like landslides or tectonic motion on the watershed. In fact, we show that the same type of topological perturbation can indeed trigger non-local effects of any length scale, i.e., following power-laws distributions. For illustration, as shown in Fig. 1, we obtain after a local height change of less than 2 m at a location (cross) close to the Kashabowie Provincial Park, some kilometers North of the US-Canadian border, a substantial displacement in the watershed (blue), which encloses together with the original watershed (red) an area $A \sim 3730 \text{ km}^2$. Here a model is developed to provide a qualitative and quantitative description of this phenomenon.

In our simulations, we use real and artificial landscapes in the form of Digital Elevation Maps (DEM), consisting of discretized elevation fields. Here we call *sites* to the discretization units, defined as the square areas with a size given by the DEM resolution. The watershed is the

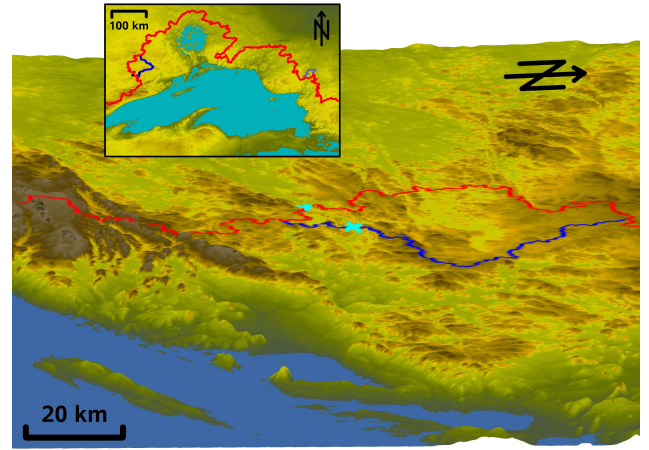


FIG. 1. (color online) Example of the watershed between US and Canada, close to the big lakes (red). Also shown is the resulting change in the watershed (blue) due to a perturbation of 2 m at a spot (cross) close to the border, near Thunder Bay. The watershed displacement encloses an area of about 3730 km^2 . The dot marks the new *outlet* of the area after perturbation. The inset shows the same area on a larger scale.

line dividing the entire landscape into two parts. Each part drains, according to the steepest descent along the coordinate directions, to either one of a chosen pair of opposite boundaries (east-west or north-south) of the DEM. For the determination of this line we use an iterative application of an invasion percolation procedure (IP) [14]. For a given landscape, as shown in Fig. 1, we initially determine its watershed (red line). Then a local event is induced by changing the height $h_k \rightarrow h_k + \Delta$ at a single site k (cross in Fig. 1) of the DEM, where Δ is the perturbation strength. Since we are interested on the non-local features of the watershed response to local perturbations, we only perturb sites that are not on the watershed. This implies $\Delta > 0$ to induce changes in the watershed (blue line). The displacement of the watershed is quantified by measuring the area A between the original and the perturbed watershed. By definition, the water can only escape from the displacement area through a single site,

which we call *outlet*. The old outlet (*o-outlet*) before perturbation always coincides with the perturbed site k . After perturbation, k becomes part of the new watershed and the water escapes through a new outlet (*n-outlet*), which is located at the original watershed. After measuring the area A and the distance R between the old and new outlets, we proceed by restoring the original landscape, i.e., the height at k is reset to its initial value. This procedure is repeated for every site k of the landscape, except those located at the original watershed. Initially, we fix Δ equal to $h_w = |h_{max} - h_{min}|$, i.e., the height difference between the lowest h_{min} and highest height h_{max} of the landscape, which corresponds to a perturbation of infinite strength for the landscape under investigation. With this choice all possible changes are obtained within the DEM. In all definitions hereafter, we consider only those perturbations leading to a displacement of the watershed. In what follows, we study the distribution $P(A)$ of the areas A , the probability distribution $P(R)$ of the Euclidean distance R between the two outlets, and the dependence between A and R . For this, we define the average area $\langle A \rangle$ and the distribution $P(A|R)$ of areas A associated with an outlet distance R .

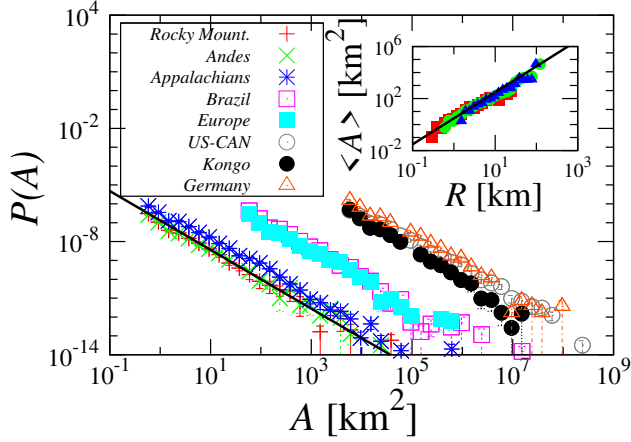


FIG. 2. (color online) The distribution $P(A)$ is shown for various regions: Rocky Mountains, Andes and Appalachian (unshifted); Brazil and Europe (shifted by a factor of 10^2 for better visibility); US-CAN, Kongo and Germany (shifted by 10^4). All data sets have a resolution of 540 m. The solid line shows the fit to the Andes data with a power-law of exponent -1.65 ± 0.15 . The inset shows $\langle A \rangle$ as function of R for the Rocky Mountains at resolutions of 270 m (squares), 540 m (circles) and 1350 m (triangles). The solid line has slope 2.

First, we study several natural landscapes, from mountainous (e.g. Rocky Mountains) to rather flat landscapes (e.g. US-CAN, Kongo and Germany). The DEM data was obtained from the SRTM-project [15], where for each set we used a size of $2700 \text{ km} \times 2700 \text{ km}$ (except $1080 \text{ km} \times 1080 \text{ km}$ for Germany), and a resolution of 540 m, defining the size of a site. Hence, the physical size of the 8 data sets are large enough, so that finite size effects emerging from the DEM boundaries could not be

detected. As shown in Fig. 2, we find the distribution of areas to follow a power-law, $P(A) \sim A^{-\beta}$, with $\beta = 1.65 \pm 0.15$ for all landscapes. The probability distribution $P(R)$ of outlet distances R also obeys a power-law, $P(R) \sim R^{-\rho}$, with $\rho = 3.1 \pm 0.3 \approx 2\beta$ (see Fig. SM1 in [16]), and displays an upper cutoff in the range $50 \text{ km} < R < 500 \text{ km}$ for the studied landscapes. This cutoff is independent on the resolution and could be due to a length scale arising from tectonics. The value of ρ implies $\langle A \rangle \sim R^2$, which agrees well with our data (inset of Fig. 2). The distribution for a given distance R scales as $P(A|R) \sim A^{-\alpha}$ with $\alpha = 2.3 \pm 0.2$ (see Fig. SM1 in [16]).

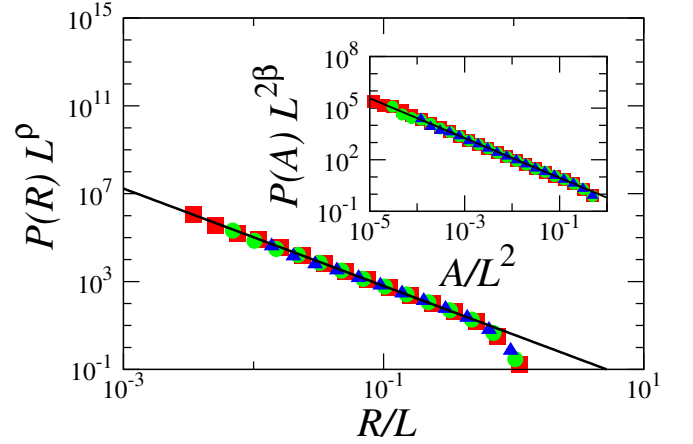


FIG. 3. (color online) Data collapse of the distribution $P(R)$ for uncorrelated landscapes ($H = -1$) of three different system sizes $L = 129, 257, 513$ (triangles, circles and squares, respectively). The line represents a power-law fit to the data for the largest landscape (squares) revealing an exponent $\rho = 2.21 \pm 0.01$. The inset shows the distribution $P(A)$ of the areas for the same system sizes. The line represents a power-law fit to the data with exponent $\beta = 1.16 \pm 0.03$.

In order to understand these power-laws and the dependence between A and R , we study artificial landscapes, where the local heights are generated using fractional Brownian motion (fBm) on a square lattice [17]. This model incorporates spatial long-range correlations to the system that are controlled by the Hurst exponent, H . We first consider the case of uncorrelated landscapes, which is a special case of the fBm model with $H = -1$. In Fig. 3, we present the results obtained for several system sizes, using the same procedure as for the natural landscapes. The probability density $P(R)$ again follows a power-law $P(R) \propto R^{-\rho}$, without upper cutoff as in real landscapes. We estimate $\rho = 2.21 \pm 0.01$ using the scaling $P(R) = L^\rho f[RL]$, where L is the linear dimension of the landscape. For the distribution $P(A) = L^\beta f[AL^2]$, we obtain an excellent data collapse for $\beta = 1.16 \pm 0.03$ (see the inset of Fig. 3). In the case of the distribution $P(A|R)$ at a fixed outlet distance, we again find a power-law $P(A|R) \sim A^{-\alpha}$ (see Fig. SM2 in [16]). Finite size scaling analysis yields an exponent $\alpha = 2.23 \pm 0.03$

independent on the value of R . Assuming that R describes the extension of A in every direction, the relation $\rho = \alpha$ is reasonable. This is even well supported by the similarity of the obtained exponents. The area A was rescaled by L^2 , indicating that the areas are compact. Considering finite-size scaling, our data is consistent with $\langle A \rangle \sim R^2$ (see Fig. SM2 in [16]). Furthermore, the compactness of the areas is supported by the measured value $\beta = 1.16 \pm 0.03$, which agrees well with the relation $\beta = \rho/2 \approx 1.11$.

In the following we show that we can match the exponents quantitatively by tuning the Hurst exponent H to introduce spatial long-range correlations, as present in real geological systems. The exponents α , β and ρ were calculated for several values of H (see Fig. 4). As shown in Fig. 4, we observe that both β and ρ increase with H . Furthermore, the relationship $\beta = \rho/2$ is maintained, since the areas remain compact in the entire range of H values. Around $H = -0.5$, α starts to deviate from ρ and for $H > 0$ we observe α to decrease. Previously, we had assumed R to reflect the extension of the area, i.e., the outlets to reside typically on opposite sides of the area. To check whether this is still valid, we measured the angle θ between the lines connecting the center of mass of the area with the two outlets. We observe the average angle to decrease as a function of H (see Fig. 4). This implies that, on average, the two outlets approach each other with increasing H (see also the insets of Fig. 4), so that R is no longer representative of the area extension. Finally we find good quantitative agreement with the exponents obtained from the natural landscapes, which are known to have a Hurst exponent inside the range $0.3 < H < 0.5$ (see Ref. [18] and references therein). Hence, except for the upper cutoff in R , our model provides an excellent quantitative description of the effects observed on natural landscapes.

Next we analyze quantitatively the impact of the perturbation strength Δ on the watershed. In Fig. 5 the number of perturbed sites N that change the watershed is shown for uncorrelated, for artificial correlated (with $H = 0.3$) and for natural landscapes (Andes). In all three cases, N is found to increase linearly with the applied perturbation strength, $N \sim \Delta$. This indicates that changes on the watershed can be observed even for infinitesimally small perturbations. Additionally, in both cases where correlations are present, N is observed to reach a plateau. As already stated, when Δ is equal to h_w , this corresponds to the largest relevant perturbation, so that $N(h_w) = N_{max} \ll L^2$ indicates that many perturbations never change the watershed at all. It is clear that $\Delta > |h_j - h_i|$ is needed, where h_i and h_j are the heights of the outlets of the area. Therefore, if the distribution $p_o(h)$ of outlet heights is known, one obtains,

$$N(\Delta) = 2 \frac{N_{max}}{L^2} \int_0^\Delta \int_{\Delta'}^{h_w} p_o(h) p_o(h - \Delta') dh d\Delta' . \quad (1)$$

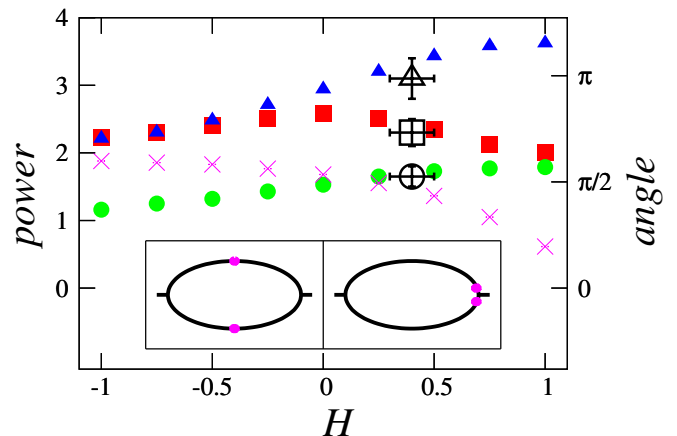


FIG. 4. (color online) The exponents α (squares), β (circles) and ρ (triangles) are shown for several values of the Hurst exponent H . Each point results from a similar study as done for the uncorrelated landscapes. The exponents for the natural landscapes (open symbols), all corresponding to Hurst exponent values in the range $0.3 < H < 0.5$, are consistent with our model. The average angle θ (in radians) between the outlets from the center of mass is shown too (crosses). The insets depict schematic shapes of the areas and positions of the two outlets for small (left) and large (right) values of H .

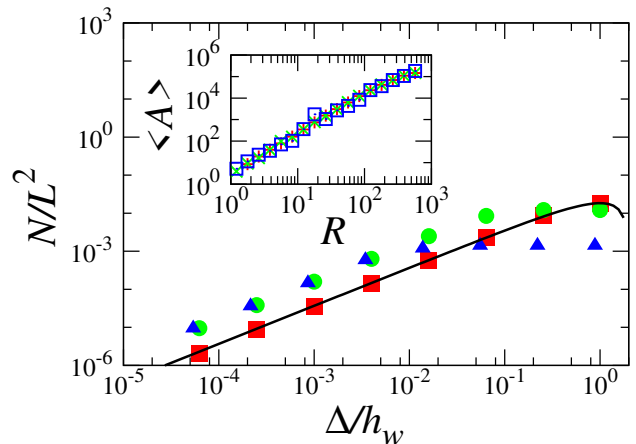


FIG. 5. (color online) Dependence of the number of perturbed sites N that promote changes on the watershed on the perturbation strength Δ applied for uncorrelated (squares), Andes (triangles) and fBm landscape with $H = 0.3$ (circles). The solid line corresponds to the analytic relation obtained from Eq. (1) for uncorrelated landscapes. The inset shows the average area $\langle A \rangle$ as a function of the distance R between the outlets for $\Delta/h_w = 1, 0.016$ and 0.00025 (pluses, crosses, and squares, respectively), and $L = 513$.

For landscapes with uniformly distributed heights, we find $p_o(h)$ to be still a uniform distribution. Then we obtain from Eq. (1), $N(\Delta) = (h_w \Delta - \Delta^2/2) 2N_{max}/(L^2 h_w^2)$, which is in excellent agreement with our data (see Fig. 5), where an approximately linear behavior can be observed for $\Delta < h_w$. The observed power-laws are maintained for all values of Δ , as can be clearly seen for $\langle A \rangle$ in the

inset of Fig. 5. We conclude that infinitesimally small perturbations have qualitatively the same effect on the watershed as any larger perturbation strength Δ .

In the case of uncorrelated landscapes ($H = -1$), for a given area A , the corresponding invasion percolation cluster is obtained by starting the penetration process from one outlet to another, always growing along the steepest descent. The area A can therefore be understood as the envelop of this IP-cluster. From percolation theory, the fractal dimension of the IP cluster is $d_f = 91/48$ in two dimensions [19], which implies that $\langle A \rangle \propto M^{2/d_f}$, where M is the number of sites (mass) of the cluster. This result is consistent with our simulations. The size-distribution $P(M|R)$ of IP-clusters between two sites at a fixed distance R is known to follow a power-law $M^{-\alpha^*}$ with $\alpha^* = 1.39$ [19]. Note that, for comparison of our results to Araújo *et al.* [19], $P(M|R)$ needs to be divided by M , as we grow the IP-cluster starting from the outlet at the watershed, which is always the highest of the M sites of the cluster. Hence we expect $P(M|R) \sim M^{-(\alpha^*+1)}$, what is indeed in good agreement with our data (see Fig. SM3 in [16]). We can now relate our exponent α of the distribution of areas at fixed distance to α^* , which describes the size-distribution of IP-clusters, as $P(A|R) = P(\langle A \rangle(M)|R) \propto \langle A \rangle^{-\alpha}(M) \propto M^{2\alpha/d_f} \propto P(M|R)$. We obtain $\alpha = \frac{d_f}{2}(\alpha^* + 1) \approx 2.266$, which is very close to what we measure ($\alpha = 2.23 \pm 0.03$). Therefore, we can relate our results on uncorrelated landscapes to the subcritical point-to-point invasion percolation process [19] and to the mass distribution of avalanches that occur during the IP-cluster growth [20–22].

In summary, we were able to show that small and localized perturbations can have a large impact on the shape of watersheds even at very long distances, hence having a non-local effect. The distribution of changes $P(A)$ is found to decrease as a power-law with exponent $\beta = 1.65 \pm 0.15$ on all studied real landscapes from mountainous (e.g. Rocky Mountains) to rather flat (e.g. US-Canadian border). By applying perturbations to model landscapes with long-range correlations, we determined the dependence of the scaling exponents on the Hurst exponent, finding good quantitative agreement with real landscapes, for which $0.3 < H < 0.5$. The obtained exponents α , β and ρ are independent of the perturbation strength Δ . For uncorrelated landscapes, we derived a relation with invasion percolation. It is known that watersheds [14] on uncorrelated landscapes are related to “strands” in Invasion Percolation [23], random polymers in strongly disordered media [24], paths on MST’s [25], the backbone of the optimal path crack [26] and the cluster perimeter in explosive percolation [27]. Hence, our results can be potentially applied to all these problems.

We acknowledge useful discussions with N. A. M. de Araújo and thank CNPq, CAPES, FUNCAP, and the CNPq/FUNCAP-Pronex grant for financial support.

* ericfehr@ethz.ch

- [1] C. J. Vorosmarty, C. A. Federer, and A. L. Schloss, *J. Hydrol.* **207**, 147 (1998); A. Y. Kwarteng *et al.*, *J. Arid. Environ.* **46**, 137 (2000); A. Sarangi, and A. K. Bhat-tacharya, *Agric. Water Manage.* **78**, 195 (2005).
- [2] A. S. Dhakal, and R. C. Sidle, *Hydrol. Processes* **18**, 757 (2004); B. Pradhan, R. P. Singh, and M. F. Buchroithner, *Adv. Space Res.* **37**, 698 (2006); M. Lazzari *et al.*, *Landslides* **3**, 275 (2006).
- [3] K. T. Lee, and Y. T. Lin, *J. Am. Water Resour. Assoc.* **42**, 1615 (2006).
- [4] P. Burlando, M. Mancini, and R. Rosso, *IFIP Trans. B* **16**, 91 (1994); D. Q. Yang *et al.*, *J. Geophys. Res. Earth Surf.* **112**, F02S22 (2007).
- [5] http://untreaty.un.org/cod/riaa/cases/vol_IX/29-49.pdf
- [6] L. Vincent, and P. Soille, *IEEE T. Pattern. Anal.* **13**, 583 (1991); P. P. Bruyant, and M. A. King, *J. Nucl. Med.* **43**, 206P (2002); Y. Ikeda *et al.*, *Med. Phys.* **34**, 4378 (2007).
- [7] C. P. Burrridge, D. Craw, and J. M. Waters, *Mol. Ecol.* **16**, 1883 (2007).
- [8] D. Garcia-Castellanos *et al.*, *Nature* **462**, 778 (2009).
- [9] R. Linkeviciene, *Holocene* **19**, 1233 (2009).
- [10] R. J. Dorsey and J. J. Roering, *Geomorphology* **73** (1-2), 16 (2006); J. Look, H. Kelsey, K. Furlong and A. Woolace, *Geol. Soc. Am. Bull.* **118** (9-10), 1232 (2006); L. P. Beranek, P. K. Link and C. M. Fanning, *Geol. Soc. Am. Bull.* **118** (9-10), 1027 (2006).
- [11] P. Bishop, *Prog. Phys. Geog.* **19**, 449 (1995).
- [12] M. Attal *et al.*, *J. Geophys. Res. Earth Surf.* **113**, F03013 (2008); J. Douglass and M. Schmееckle, *Geomorphology* **84**, 22 (2007).
- [13] C. M. Patil and S. Patilkulkarni, *IEEE Proceedings of ARTCom 2009*, p. 796 (2009); J. K. Dixon, *IEEE T. Syst. Man Cyb.* **9** (10), 617 (1979).
- [14] E. Fehr *et al.*, *J Stat Mech-Theory E*, P09007 (2009).
- [15] Farr T G *et al.*, *Rev. Geophys.* **45**, RG2004 (2007).
- [16] See supplementary material at <http://link.aps.org/>.
- [17] K. B. Lauritsen, M. Sahimi and H. J. Herrmann, *Phys. Rev. E* **48**, 1272 (1993).
- [18] R. Pastor-Satorras and D. H. Rothman, *Phys. Rev. Lett.* **80**, 4349 (1998).
- [19] A. D. Araujo *et al.*, *Phys. Rev. E* **72**, 041404 (2005).
- [20] J. Lomnitz-Adler *et al.*, *Phys. Rev. A* **45** (4), 2211 (1992).
- [21] L. A. N. Amaral *et al.*, *Phys. Rev. E* **51** (5), 4655 (1995).
- [22] M. Ferer *et al.*, *Physica A* **311** (1-2), 5 (2002).
- [23] M. Cieplak, A. Maritan and J. R. Banavar, *Phys. Rev. Lett.* **76**, 3754 (1996).
- [24] M. Porto *et al.*, *Phys. Rev. E* **60**, R2448 (1999).
- [25] R. Dobrin and P. M. Duxbury, *Phys. Rev. Lett.* **86**, 5076 (2001).
- [26] J. S. Andrade *et al.*, *Phys. Rev. Lett.* **103**, 225503 (2009).
- [27] N. A. M. Araújo and H. J. Herrmann, *Phys. Rev. Lett.* **105**, pp. 035701 (2010).